

B_c , B_s and D_s production at lepton-hadron colliders

Qi-Wei Hu¹, Cong-Feng Qiao^{1,*} and Li-Ping Sun²

¹*School of Physics, University of Chinese Academy of Sciences, Beijing 100049, China and*

²*School of Science, Beijing University of Civil*

Engineering and Architecture, Beijing 100044, China

Abstract

Within the framework of nonrelativistic quantum chromodynamics, this study examines the electroproduction processes $e + p \rightarrow e + B_c + \bar{c} + b$, $e + p \rightarrow e + B_s + \bar{s} + b$, and $e + p \rightarrow e + D_s + \bar{c} + s$ at lepton-hadron colliders. The differential cross sections in $\cos \theta$ and p_T^2 at HERA are presented. The results indicate that the production of B_c is feasible at the EIC, whereas it is not at HERA. The cross sections for B_s and D_s are notably significant at HERA, yet they exhibit sensitivity to variations in quark mass and renormalization scale.

* Corresponding author: qiaocf@ucas.ac.cn

I. INTRODUCTION

The field of heavy quarkonium research originated with the 1974 discovery of charmonium J/ψ [1, 2], followed by the 1977 identification of bottomium Υ at Fermilab [3]. Heavy quarkonium serves as an exemplary system for quantum chromodynamics (QCD) research. The low relative velocity of quarks within heavy quarkonium allows for the factorization of scattering amplitudes into hadronization and perturbative components. Based on this property, nonrelativistic quantum chromodynamics (NRQCD) [4] is pivotal in addressing the production and decay processes of these systems.

The B_c meson stands out among mesons for its composition of two distinct heavy flavor quarks, leading to decay processes governed solely by weak interactions. This characteristic offers a unique opportunity to probe quark weak interactions. Despite its small production cross section, the S-wave ground state $B_c(^1S_0)$ was first observed in 1998 at Tevatron by the CDF collaboration [5]. Within the B_c family, the S-wave vector state $B_c^*(^3S_1)$ [6] decays predominantly into B_c , underscoring the significance of B_c^* in B_c -related processes.

Production of B_c can be categorized as either direct or indirect. Direct production refers to production at colliders by partons, e^\pm , $\gamma^{(*)}$, etc. Indirect production involves the decay of massive intermediate particles such as W^\pm , Z , H , and t into B_c . At ep colliders, B_c production is further differentiated into photoproduction and electroproduction. Photoproduction involves the initial photon being emitted through electron bremsstrahlung, with energy distribution described by the Weizsäcker-Williams approximation [7]. Laser back scattering (LBS) can generate photons with higher energy due to significant electron energy transfer [8]. Electroproduction, which involves electron interaction with a gluon via a virtual photon, is the focus of this study.

The LHC, with its record collision energy and extensive data, has made strong production a focal point since its inception. The leading order (LO) calculations for B_c strong production, which began in the 1990s [9, 10], have concentrated on S-wave B_c production at hadron colliders, including the Tevatron and LHC. For higher excited state B_c mesons under the NRQCD framework, Ref. [11] calculated P-wave B_c strong production, while Ref. [12] examined the color octet mechanism (COM) in B_c strong production. Ref. [13] also provided a detailed analysis of B_c strong production driven by intrinsic heavy quarks within

colliding hadrons. Note, the heavy quark fragmentation method [14, 15] is also widely used in production of mesons with b or c quark, including B , D and D_s families [16, 17].

Beyond strong production, B_c can also arise from electron-positron collisions, electron-proton collisions, and heavy-ion collisions. Ref. [18] analyzed B_c production in Z factory, encompassing S-wave, P-wave, and color octet states. Refs. [19, 20] calculated the double photon production of S-wave and P-wave B_c , revealing that differential distributions under NRQCD and fragmentation methods are markedly different. At ep colliders, B_c can be produced through interactions involving photons and gluons [21]. At the LHC, heavy-ion Pb + Pb collisions can also yield B_c [22, 23].

Compared to pp colliders, ep colliders operate at lower energies but offer higher luminosities and distinct scientific goals. The HERA [24] has ceased operations, while the EIC [25, 26] and EIC [27] are currently under construction. The EIC, in contrast to HERA, operates at lower energies but with higher luminosity and is capable of producing highly polarized electron and proton beams. Its design objectives include using electrons as probes to investigate the internal structure of nucleons. The results presented in this article are based on these ep colliders.

This paper aims to fill a current gap in the electroproduction of B_c and provide an estimate valuable for future collider experiments. Additionally, the production of B_s and D_s mesons are calculated to evaluate the applicability of NRQCD framework in mesons containing a single heavy quark.

II. FORMALISM

In NRQCD, the cross section can be decomposed as follows:

$$\begin{aligned} d\sigma(ep \rightarrow e + M + q + \bar{q}') &= \int dx f_{g/p}(x, \mu^2) \\ &\times d\sigma(eg \rightarrow e + q\bar{q}' [n] + q + \bar{q}') \langle \mathcal{O}^M(n) \rangle, \end{aligned} \quad (1)$$

where M is the final meson, q and \bar{q}' is the component quark of meson, $\langle \mathcal{O}^M(n) \rangle$ represents the long-distance matrix element (LDME), $n = {}^{2S+1}L_J$ is the standard spectroscopic notation for the quantum number of the $q\bar{q}'$ pair, and $f_{g/p}(x, \mu^2)$ is the parton distribution function (PDF) of gluon evaluated at the factorization scale μ^2 .

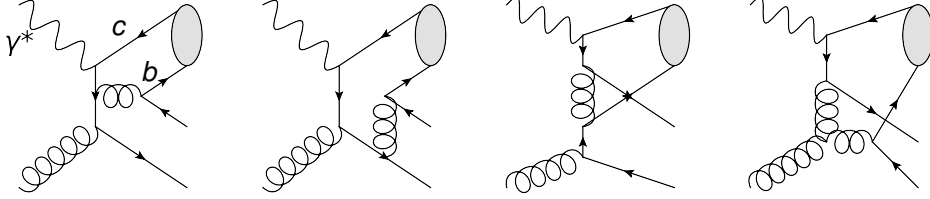


FIG. 1. Typical LO Feynman diagrams of $\gamma^* + g \rightarrow B_c + \bar{c} + b$.

Furthermore, for electroproduction, the leptonic tensor formula [28] can formally reduce the number of Mandelstam invariants:

$$\begin{aligned} d\sigma(eg \rightarrow e + q\bar{q}'[n] + q + \bar{q}') = \\ \frac{1}{4xP \cdot k} \frac{1}{N_c N_s} \frac{1}{(Q^2)^2} L_{\mu\nu} H^{\mu\nu}[n] d\text{PS}_4. \end{aligned} \quad (2)$$

The notation follows the reference, N_c and N_s are the color and spin number, P and k are momentum of initial proton and electron, Q^2 is the virtuality of γ^* , $L_{\mu\nu}$ is the leptonic tensor for the initial electron emitting a virtual photon, $H^{\mu\nu}[n]$ is the hadronic part of the interaction between the virtual photon and the gluon, and $d\text{PS}_4$ is the 4 body phase space for $e + B_c + b + \bar{c}$. To improve the efficiency, the phase space can be decomposed:

$$\begin{aligned} \int d\text{PS}_4 = (2\pi)^2 \int_{4m^2}^{E^2} dP_{B_c b \bar{c}}^2 d\text{PS}_2(e + g \rightarrow e + [B_c b \bar{c}]) \times \\ \int_{m^2}^{M^2} dP_{b \bar{c}}^2 d\text{PS}_2([B_c b \bar{c}] \rightarrow B_c + [b \bar{c}]) d\text{PS}_2([b \bar{c}] \rightarrow b + \bar{c}), \end{aligned} \quad (3)$$

where $d\text{PS}_2$ is the two body phase space, $m = m_b + m_c$, E is the collision energy, P_X is the four momentum of the system X , and $M = \sqrt{P_{B_c b \bar{c}}^2} - m$.

The $q\bar{q}'$ pair hadronization process can be computed using the covariant projection operator method. For pseudoscalar, the projection operator can be expressed as:

$$\frac{1_c}{\sqrt{N_c}} \otimes \frac{1}{2\sqrt{M}} \gamma_5 (\not{P} + m_1 + m_2), \quad (4)$$

where 1_c is the identity matrix in color space, M and P are the mass and momentum of the meson, respectively, and m_1 and m_2 are the masses of the constituent quarks. For vector mesons, just replace γ_5 with $\not{\epsilon}$.

Typical LO Feynman diagrams are shown in Fig. 1. All the 24 diagrams can be generated by varying the gluon and photon, reversing fermion lines, and considering different quark

pairs for the meson. For bc and cs pairs, the same analytical amplitude are used, adjusting only the corresponding quark masses during the Monte Carlo simulation. For bs pair, although the 24 diagrams appear identical to those of bc and cs , the color algebra structure differs, resulting in a distinct analytical amplitude.

The following packages are applied in calculations:

- FeynArts [29]: for generating Feynman diagrams
- FeynCalc [30]: for generating analytical amplitude expressions and performing SU(3) color algebra
- CUBA [31]: for numerically calculating the phase space integral

FeynCalc seems to give wrong results when contracting long chains of Dirac gamma matrix, and can be solved by manually add contracting rules.

III. RESULTS

The electron mass and the mass split between vector and pseudoscalar mesons are neglected in calculation. Quark masses are set as

$$m_c = 1.5 \text{ GeV}, m_b = 4.9 \text{ GeV}, m_s = 0.5 \text{ GeV}, \quad (5)$$

for B_c , B_s , and D_s .

The running coupling constant uses the one-loop formula at LO. For charm mesons, the number of quark flavors $n_f = 4$, and the QCD scale $\Lambda_{\text{QCD}} = 297 \text{ MeV}$. For bottom mesons, $n_f = 5$, and $\Lambda_{\text{QCD}} = 214 \text{ MeV}$ [32]. The renormalization scale μ is set to $\mu = m_T = \sqrt{M^2 + p_T^2}$, where M , m_T , and p_T are the mass, transverse mass, and transverse momentum of the meson, respectively. To estimate the uncertainty, μ is set within the range of $\frac{1}{2}m_T < \mu < 2m_T$, and the quark mass is adjusted within the range of $\pm 0.1 \text{ GeV}$ with the meson mass held constant. Notably, the result specifically isolates the uncertainties arising solely from mass variations. The relationship between the LDME and the wave function at the origin of the meson is $\langle \mathcal{O}^M \rangle = 2(2J + 1)N_c |R(0)|^2 / 4\pi$. Similar to J/ψ , the LDME can

be extracted from the meson decay width. However, since the quark flavors are different, the width here is from weak decay, proportional to the corresponding decay constant f^2 [32]:

$$\Gamma^0(P \rightarrow l\nu) = \frac{G_F^2}{8\pi} f_P^2 m_l^2 M_P \left(1 - \frac{m_l^2}{M_P^2}\right)^2 |V_{q_1 q_2}|^2, \quad (6)$$

where M_P and f_P is the mass and decay constant of the pseudoscalar meson, m_l is the final lepton mass, $|V_{q_1 q_2}|$ is the Cabibbo-Kobayashi-Maskawa (CKM) matrix element between the quarks in the pseudoscalar meson, and G_F is the Fermi coupling constant. The relationship between f_P and $|R(0)|$ is

$$f_P^2 = N_c |R(0)|^2 / \pi M_P. \quad (7)$$

For B_c , the wave function can be directly calculated from the Buchmüller-Tye potential [33, 34]. For B_s and D_s , the wave functions are obtained from the decay constant. PDG [32] provides the decay constants $f_{B_s} = 0.234$ GeV and $f_{D_s} = 0.245$ GeV, which are determined from a combination of experimental measurements and lattice QCD calculations. Finally, at leading order:

$$\begin{aligned} |R_{B_c}(0)|^2 &= 1.642 \text{ GeV}^3, & |R_{B_c^*}(0)| &= |R_{B_c}(0)|, \\ |R_{B_s}(0)|^2 &= 0.299 \text{ GeV}^3, & |R_{B_s^*}(0)| &= |R_{B_s}(0)|, \\ |R_{D_s}(0)|^2 &= 0.124 \text{ GeV}^3, & |R_{D_s^*}(0)| &= |R_{D_s}(0)|. \end{aligned} \quad (8)$$

According to NRQCD heavy quark spin symmetry at leading order in v [4], pseudoscalar and vector mesons share the same $R(0)$. For the PDF, CT10 [35] is used.

The collision parameters and experimental cuts are taken from HERA: the electron energy is 27.5 GeV, the proton energy is 920 GeV, $p_T > 1$ GeV, and $0.3 < z < 0.9$. The electroproduction photon virtuality is set as $2 \text{ GeV}^2 < Q^2 < 100 \text{ GeV}^2$. Given that the production cross section for B_c is much smaller than that for J/ψ , $50 \text{ GeV} < W < 250 \text{ GeV}$ is relatively broader than the constraints employed at HERA. $W = \sqrt{(p_\gamma^2 + p_P^2)}$ is the mass of the hadronic final state, $z = (p_1 \cdot p_P) / (p_\gamma \cdot p_P)$ is the elasticity of the meson production process, and p_1, p_P, p_γ are the momenta of the meson, proton, and photon, respectively.

The $\cos \theta$ and p_T^2 distributions of the B_c and B_c^* production cross sections are shown in Fig. 2, where θ is the angle between the meson and the incident electron. The cross section of B_c^* is much larger than that of B_c , demonstrating its significance in B_c associated

processes. As expected, the $\cos\theta$ distribution is concentrated in the incident proton direction $\cos\theta = -1$, and decreases rapidly as $\cos\theta$ increases. To be precise, the area of $\cos\theta \lesssim -0.4$ and $p_T^2 \lesssim 30 \text{ GeV}^2$ is dominant. On the other hand, data at large $\cos\theta$ or p_T^2 are too small and may be severely affected by Monte Carlo errors. Nevertheless, disregarding the minor data fluctuations, the B_c^* differential cross section decreases more rapidly compared to that of B_c .

The total LO B_c and B_c^* cross sections are

$$\begin{aligned}\sigma_{B_c} &= 42.13_{-4.88-14.77}^{+6.38+38.14} \text{ fb}, \\ \sigma_{B_c^*} &= 164.17_{-18.35-58.65}^{+23.49+151.34} \text{ fb},\end{aligned}\tag{9}$$

where the former uncertainty are from quark mass only, and the latter one combined with the former one represent the overall uncertainty. In the case of B_c , the mass uncertainty only accounts for a minor fraction of the total uncertainty.

It is not surprising that the number of B_c events detected by HERA is insufficient. The production cross section of bottom mesons is generally two to three orders of magnitude lower than that of charm mesons, and the reconstruction efficiency is also smaller. Although most of B_c^* decay into B_c , the branching ratio of $B_c^\pm \rightarrow J/\psi\pi^\pm \approx 0.5\%$ [36] is too small to generate enough events for reconstruction. At future colliders with higher energy or luminosity, sufficient B_c events might be attainable. The ep colliders under planning include EIC and EicC, both of which are high luminosity colliders with polarized beams. Given that the EicC is designed to probe the small x region of PDF, with electron energy of 5 GeV and proton energy of 26 GeV, the cross section is $\lesssim 0.03 \text{ fb}$, thus no B_c will be observed at EicC. According to EIC yellow report [25], the unpolarized LO cross sections are calculated under electron energy 10 GeV, proton energy 275 GeV. The cut-off is $Q^2 > 1 \text{ GeV}^2$, $p_T > 1 \text{ GeV}$, $20 \text{ GeV} < W < 80 \text{ GeV}$, $0.05 < z < 0.9$, and alternative selections could be made. The results are as follows:

$$\begin{aligned}\sigma_{B_c}^{\text{EIC}} &= 5.44_{-1.03-1.91}^{+0.39+6.36} \text{ fb}, \\ \sigma_{B_c^*}^{\text{EIC}} &= 22.12_{-4.37-7.8}^{+1.07+25.6} \text{ fb}.\end{aligned}\tag{10}$$

Taking luminosity $10^{34} \text{ cm}^{-2}\text{s}^{-1} \approx 315 \text{ fb}^{-1}\text{year}^{-1}$ and that all B_c^* decays into B_c , $3922 \sim 19209 B_c$ are produced per year. Again, assuming that B_c is reconstructed through $B_c^\pm \rightarrow$

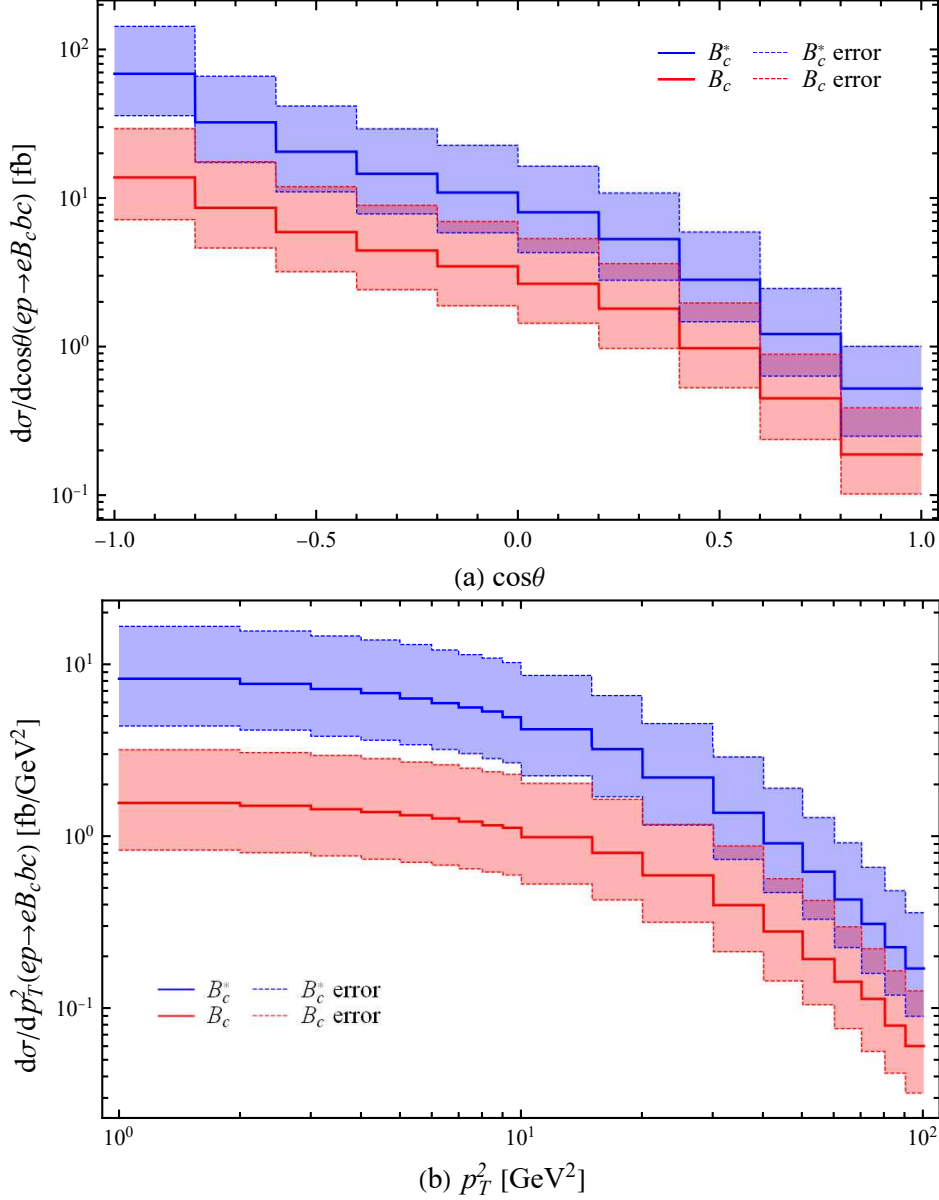


FIG. 2. The differential cross section in (a) $\cos\theta$ and (b) p_T^2 distributions of the electroproduction process $e+g \rightarrow e+B_c+\bar{c}+b$ at LO. Blue lines represent the vector B_c^{*+} , and red lines represent the pseudoscalar B_c^+ . The upper bound corresponds to $m_c = 1.4$ GeV, $m_b = 5.0$ GeV, and $\mu = \frac{1}{2}m_T$. The lower bound corresponds to $m_c = 1.6$ GeV, $m_b = 4.8$ GeV, and $\mu = 2m_T$.

$J/\psi\pi^\pm$, with a branching ratio of 0.5%. Then, for electroproduction, J/ψ can be reconstructed through $J/\psi \rightarrow l^+l^-$ ($l = e, \mu$), and the branching ratio is 12% [32] for e and μ combined. Finally, doubling the events since there are B_c^+ and B_c^- , about 5 \sim 28 events can be detected per year at EIC. With the following upgrades of high-luminosity EIC (HL-EIC)

[26], the luminosity can increase by approximately an order of magnitude and the electron beam energy can reach 16 GeV without affecting the luminosity. In summary, observing B_c at EIC is promising.

In the framework of NRQCD, the electroproduction cross sections of D_s and B_s at HERA are also calculated. Due to the light s quark component, the LO cross section and its uncertainty are significantly enhanced compared to B_c . Since m_s is about 0.5 GeV only, the variation in quark mass is constrained within the range of ± 30 MeV. However, this sensitivity to quark masses may serve as a window for experimental measurements. For example, in the case of B_s , although the total mass is 5.4 GeV, a quark mass variation of 0.1 GeV is sufficient to induce a significant change greater than 200% in the cross section.

The total LO cross sections at HERA are

$$\begin{aligned}
 \sigma_{B_s} &= 0.29_{-0.05-0.09}^{+0.06+0.25} \text{ pb}, \\
 \sigma_{B_s^*} &= 0.73_{-0.12-0.23}^{+0.15+0.63} \text{ pb}, \\
 \sigma_{D_s} &= 9.35_{-1.33-3.03}^{+1.71+5.13} \text{ pb}, \\
 \sigma_{D_s^*} &= 20.78_{-2.98-2.8}^{+3.80+11.74} \text{ pb}.
 \end{aligned} \tag{11}$$

And the differential cross section distributions are shown in Fig. 3 and Fig. 4. Their trends are analogous to B_c yet with broader error bands. In subsequent studies, the precision can be enhanced by incorporating NLO calculations and more thorough analyses.

Using an integrated luminosity of $\mathcal{L} = 315 \text{ pb}^{-1}$, $48 \sim 189 B_s^0$, $119 \sim 476 B_s^*$, $1575 \sim 5100 D_s^+$, $3465 \sim 11440 D_s^{*+}$ are produced at HERA. Considering the high reconstruction efficiency, these events are sufficient for analysis of the main decay channels. Nevertheless, for the investigation of rare decay channels including Cabibbo-suppressed modes, more events must be acquired at future colliders.

IV. CONCLUSION AND OUTLOOK

In this paper, the electroproduction of B_c , B_s , and D_s at ep colliders at LO are investigated within the framework of NRQCD. The results indicate that B_c is observable at EIC. While B_s and D_s events are abundant, their theoretical LO cross sections derived from

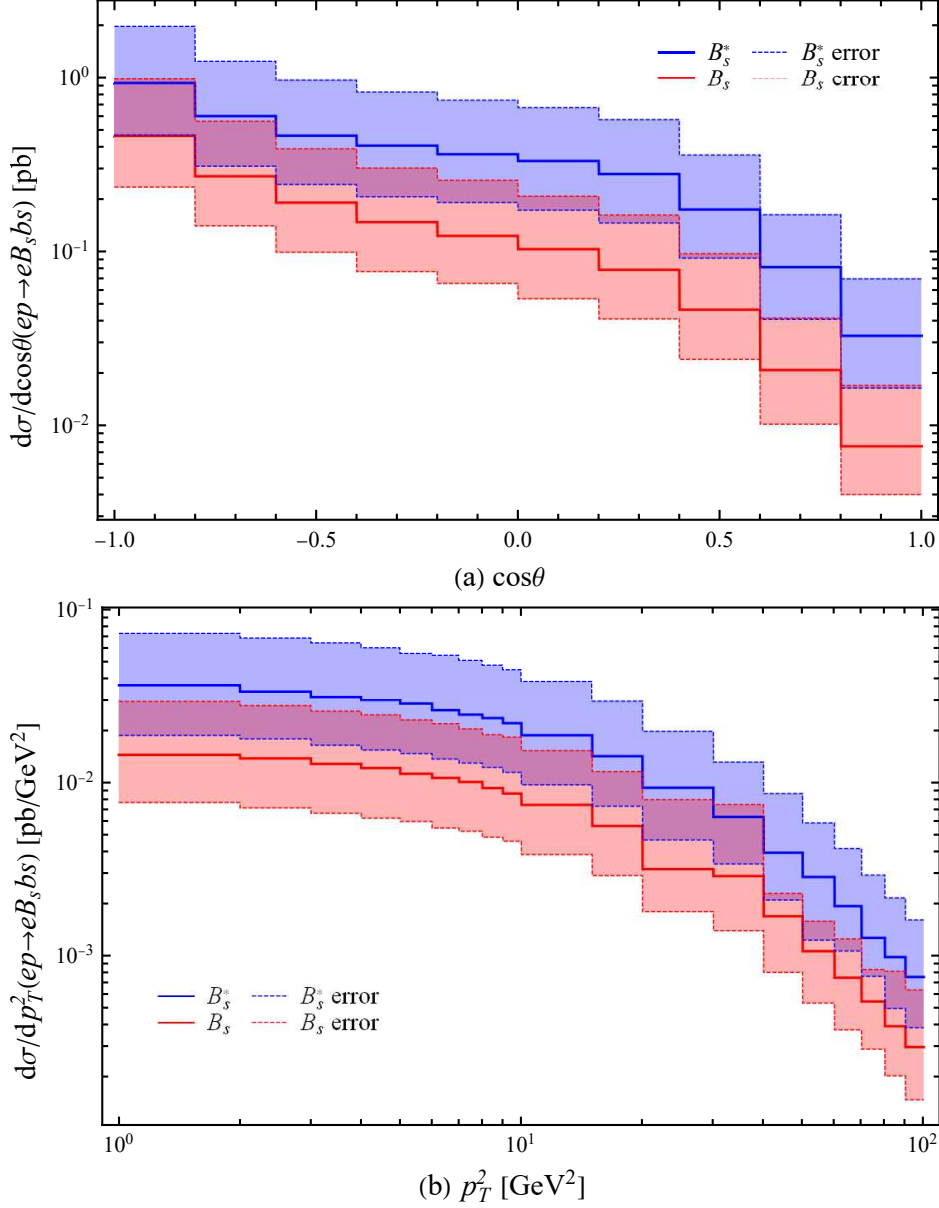


FIG. 3. The differential cross section in (a) $\cos\theta$ and (b) p_T^2 distributions of the electroproduction process $e + g \rightarrow e + B_s + \bar{s} + b$ at LO. Blue lines represent the vector B_s^* , and red lines represent the pseudoscalar B_s^0 . The upper bound corresponds to $m_s = 0.47$ GeV, $m_b = 4.93$ GeV, and $\mu = \frac{1}{2}m_T$. The lower bound corresponds to $m_s = 0.53$ GeV, $m_b = 4.87$ GeV, and $\mu = 2m_T$.

NRQCD are more dependent on parameters compared to mesons with two heavy flavors. This sensitivity can also present an opportunity in experiment. The differential cross sections in $\cos\theta$ and p_T^2 are also presented, and the production is dominant for $p_T^2 \lesssim 30$ GeV² and $\cos\theta \lesssim -0.4$. The LO uncertainty limits the accuracy of theoretical predictions, which

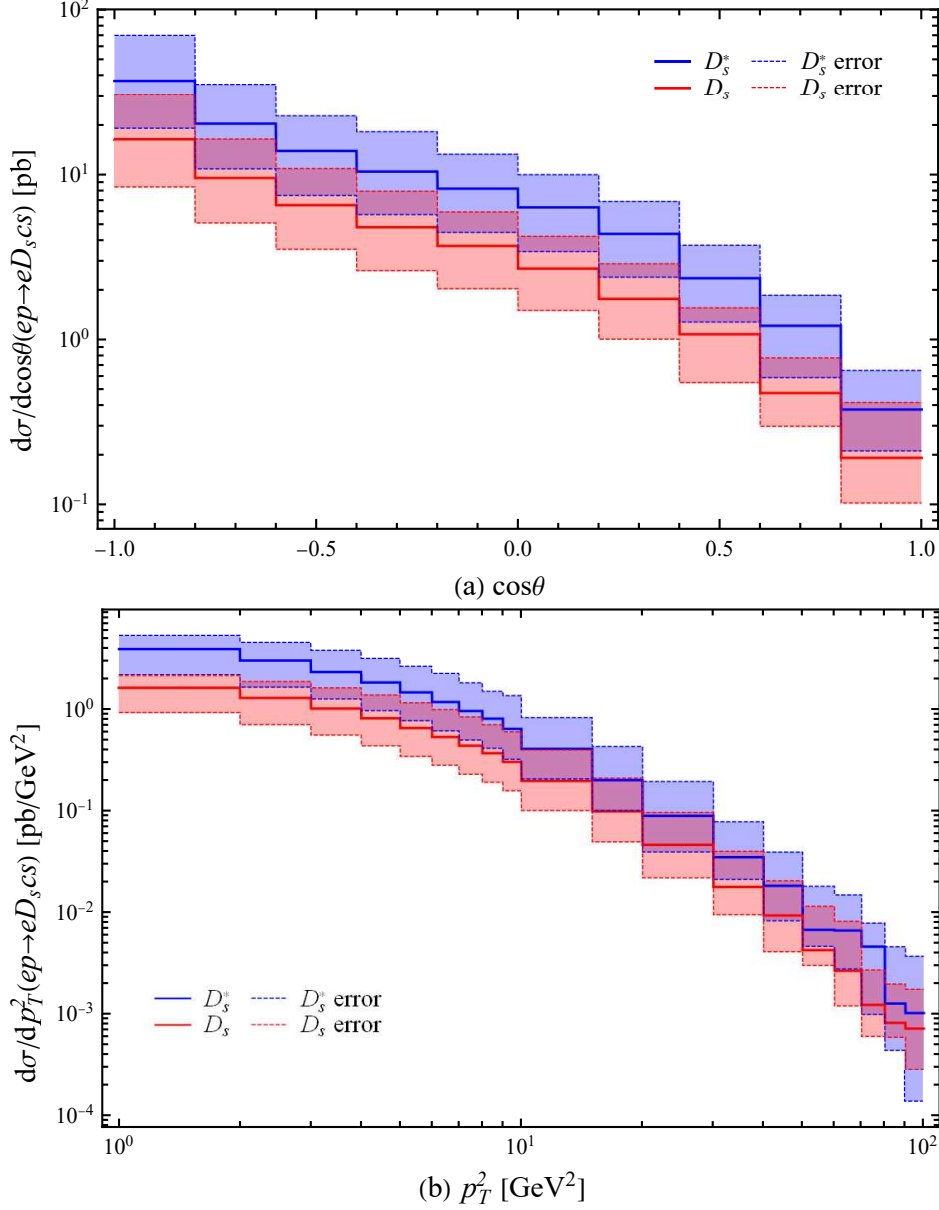


FIG. 4. The differential cross section in (a) $\cos\theta$ and (b) p_T^2 distributions of the electroproduction process $e + g \rightarrow e + D_s + \bar{c} + s$ at LO. Blue lines represent the vector D_s^{*+} , and red lines represent the pseudoscalar D_s^+ . The upper bound corresponds to $m_s = 0.47$ GeV, $m_c = 1.53$ GeV, and $\mu = \frac{1}{2}m_T$. The lower bound corresponds to $m_s = 0.53$ GeV, $m_c = 1.47$ GeV, and $\mu = 2m_T$.

can be reduced in future NLO calculations. At future high-luminosity ep or ee colliders, it is hopeful to accumulate sufficient and clean data for detailed analyses including polarization distributions and rare decay channels, which are crucial for testing NRQCD and exploring new physics.

ACKNOWLEDGEMENTS

This work was supported in part by the National Natural Science Foundation of China(NSFC) under the Grants 12235008 and 12475087.

- [1] J. J. Aubert *et al.* [E598], “Experimental Observation of a Heavy Particle J ,” Phys. Rev. Lett. **33** (1974), 1404-1406
- [2] J. E. Augustin *et al.* [SLAC-SP-017], “Discovery of a Narrow Resonance in e^+e^- Annihilation,” Phys. Rev. Lett. **33** (1974), 1406-1408
- [3] S. W. Herb *et al.* [E288], “Observation of a Dimuon Resonance at 9.5 GeV in 400 GeV Proton-Nucleus Collisions,” Phys. Rev. Lett. **39** (1977), 252-255
- [4] G. T. Bodwin, E. Braaten and G. P. Lepage, “Rigorous QCD analysis of inclusive annihilation and production of heavy quarkonium,” Phys. Rev. D **51** (1995), 1125-1171 [erratum: Phys. Rev. D **55** (1997), 5853] [arXiv:hep-ph/9407339 [hep-ph]].
- [5] F. Abe *et al.* [CDF], “Observation of the B_c meson in $p\bar{p}$ collisions at $\sqrt{s} = 1.8$ TeV,” Phys. Rev. Lett. **81** (1998), 2432-2437 [arXiv:hep-ex/9805034 [hep-ex]].
- [6] G. Aad *et al.* [ATLAS], “Observation of an Excited B_c^\pm Meson State with the ATLAS Detector,” Phys. Rev. Lett. **113** (2014) no.21, 212004 [arXiv:1407.1032 [hep-ex]].
- [7] S. Frixione, M. L. Mangano, P. Nason and G. Ridolfi, “Improving the Weizsacker-Williams approximation in electron-proton collisions,” Phys. Lett. B **319** (1993), 339-345 [arXiv:hep-ph/9310350 [hep-ph]].
- [8] I. F. Ginzburg, G. L. Kotkin, V. G. Serbo and V. I. Telnov, “COLLIDING GAMMA E AND GAMMA GAMMA BEAMS ON THE BASIS OF SINGLE COLLISION ELECTRON POSITRON ACCELERATORS. (IN RUSSIAN),” Yad. Fiz. **38** (1983), 372-384
- [9] C. H. Chang and Y. Q. Chen, “Hadronic production of the B_c meson at TeV energies,” Phys. Rev. D **48** (1993), 4086-4091
- [10] C. H. Chang, Y. Q. Chen, G. P. Han and H. T. Jiang, “On hadronic production of the B(c) meson,” Phys. Lett. B **364** (1995), 78-86 [arXiv:hep-ph/9408242 [hep-ph]].

- [11] C. H. Chang, J. X. Wang and X. G. Wu, “Hadronic production of the P-wave excited B_c -states($B_{cJ,L=1}^*$),” Phys. Rev. D **70** (2004), 114019 [arXiv:hep-ph/0409280 [hep-ph]].
- [12] C. H. Chang, C. F. Qiao, J. X. Wang and X. G. Wu, “The Color-octet contributions to P-wave B_c meson hadroproduction,” Phys. Rev. D **71** (2005), 074012 [arXiv:hep-ph/0502155 [hep-ph]].
- [13] C. H. Chang, C. F. Qiao, J. X. Wang and X. G. Wu, “Hadronic production of $B_c(B_c^*)$ meson induced by the heavy quarks inside the collision hadrons,” Phys. Rev. D **72** (2005), 114009 [arXiv:hep-ph/0509040 [hep-ph]].
- [14] B. Mele and P. Nason, Nucl. Phys. B **361** (1991), 626-644 [erratum: Nucl. Phys. B **921** (2017), 841-842]
- [15] E. Braaten, K. m. Cheung and T. C. Yuan, “Perturbative QCD fragmentation functions for B_c and B_c^* production,” Phys. Rev. D **48** (1993) no.11, R5049 [arXiv:hep-ph/9305206 [hep-ph]].
- [16] B. A. Kniehl, G. Kramer, I. Schienbein and H. Spiesberger, Phys. Rev. Lett. **96** (2006), 012001 [arXiv:hep-ph/0508129 [hep-ph]].
- [17] M. Cacciari, S. Frixione, N. Houdeau, M. L. Mangano, P. Nason and G. Ridolfi, JHEP **10** (2012), 137 [arXiv:1205.6344 [hep-ph]].
- [18] Z. Yang, X. G. Wu, G. Chen, Q. L. Liao and J. W. Zhang, “ B_c Meson Production around the Z^0 Peak at a High Luminosity e^+e^- Collider,” Phys. Rev. D **85** (2012), 094015 [arXiv:1112.5169 [hep-ph]].
- [19] K. Kolodziej, A. Leike and R. Ruckl, “Production mechanisms for B(c) mesons in photon-photon collisions,” Phys. Lett. B **348** (1995), 219-225 [arXiv:hep-ph/9412249 [hep-ph]].
- [20] A. V. Berezhnoy, V. V. Kiselev and A. K. Likhoded, “Photonic production of P wave states of B(c) mesons,” Phys. Lett. B **381** (1996), 341-347 [arXiv:hep-ph/9510238 [hep-ph]].
- [21] A. V. Berezhnoy, V. V. Kiselev and A. K. Likhoded, “NonAbelian nature of asymmetry for the B(c) meson production in gluon photon interaction,” Phys. Atom. Nucl. **61** (1998), 252-259 [arXiv:hep-ph/9710429 [hep-ph]].
- [22] Y. Liu, C. Greiner and A. Kostyuk, “ B_c meson enhancement and the momentum dependence in Pb + Pb collisions at energies available at the CERN Large Hadron Collider,” Phys. Rev. C **87** (2013) no.1, 014910 [arXiv:1207.2366 [nucl-th]].
- [23] E. Norbeck, J. Nachtman and Y. Onel, “Quarkonium and B_c mesons from Pb + Pb at LHC energies,” J. Phys. Conf. Ser. **458** (2013), 012026

- [24] F. D. Aaron *et al.* [H1], “Inelastic Production of J/ψ Mesons in Photoproduction and Deep Inelastic Scattering at HERA,” *Eur. Phys. J. C* **68** (2010), 401-420 [arXiv:1002.0234 [hep-ex]].
- [25] R. Abdul Khalek, A. Accardi, J. Adam, D. Adamiak, W. Akers, M. Albaladejo, A. Al-bataineh, M. G. Alexeev, F. Ameli and P. Antonioli, *et al.* “Science Requirements and Detector Concepts for the Electron-Ion Collider: EIC Yellow Report,” *Nucl. Phys. A* **1026** (2022), 122447 [arXiv:2103.05419 [physics.ins-det]].
- [26] A. Accardi, J. L. Albacete, M. Anselmino, N. Armesto, E. C. Aschenauer, A. Bacchetta, D. Boer, W. K. Brooks, T. Burton and N. B. Chang, *et al.* “Electron Ion Collider: The Next QCD Frontier: Understanding the glue that binds us all,” *Eur. Phys. J. A* **52** (2016) no.9, 268 [arXiv:1212.1701 [nucl-ex]].
- [27] D. P. Anderle, V. Bertone, X. Cao, L. Chang, N. Chang, G. Chen, X. Chen, Z. Chen, Z. Cui and L. Dai, *et al.* “Electron-ion collider in China,” *Front. Phys. (Beijing)* **16** (2021) no.6, 64701 [arXiv:2102.09222 [nucl-ex]].
- [28] Z. Sun and H. F. Zhang, “QCD leading order study of the J/ψ leptonproduction at HERA within the nonrelativistic QCD framework,” *Eur. Phys. J. C* **77** (2017) no.11, 744 [arXiv:1702.02097 [hep-ph]].
- [29] J. Kublbeck, M. Bohm and A. Denner, “Feyn Arts: Computer Algebraic Generation of Feynman Graphs and Amplitudes,” *Comput. Phys. Commun.* **60** (1990), 165-180
- [30] R. Mertig, M. Bohm and A. Denner, “FEYN CALC: Computer algebraic calculation of Feynman amplitudes,” *Comput. Phys. Commun.* **64** (1991), 345-359
- [31] T. Hahn, “CUBA: A Library for multidimensional numerical integration,” *Comput. Phys. Commun.* **168** (2005), 78-95 [arXiv:hep-ph/0404043 [hep-ph]].
- [32] S. Navas *et al.* [Particle Data Group], “Review of particle physics,” *Phys. Rev. D* **110** (2024) no.3, 030001
- [33] E. J. Eichten and C. Quigg, “Mesons with beauty and charm: Spectroscopy,” *Phys. Rev. D* **49** (1994), 5845-5856 [arXiv:hep-ph/9402210 [hep-ph]].
- [34] W. Buchmuller and S. H. H. Tye, “Quarkonia and Quantum Chromodynamics,” *Phys. Rev. D* **24** (1981), 132
- [35] H. L. Lai, M. Guzzi, J. Huston, Z. Li, P. M. Nadolsky, J. Pumplin and C. P. Yuan, “New parton distributions for collider physics,” *Phys. Rev. D* **82** (2010), 074024 [arXiv:1007.2241 [hep-ph]].

[36] C. H. Chang and Y. Q. Chen, “The Decays of B(c) meson,” Phys. Rev. D **49** (1994), 3399-3411